

Intra nucleus accumbens adenovirus delivery of Cre recombinase in astrocyte of elovl2-flox mice alters medium spiny neurons electrophysiological properties and emotional behavior in male and female

Martinat M ¹\$, Madore C ¹\$, Varilh M ¹, Rossito M ¹, Di Miceli M ^{1,2}, Séré A ¹, Grégoire S³, Acar N³\$, Bazinet R⁴\$, Joffre C ¹\$, Delpech JC ¹\$, Fioramonti X ¹, and Layé S ¹\$*

¹ Univ. Bordeaux, INRAE, Bordeaux INP, NutriNeurO, UMR 1286, F-33000 Bordeaux, France

² Worcester Biomedical Research Group, School of Science and the Environment, University of Worcester, Worcester WR2 6AJ, UK

³ Eye and Nutrition Research Group, Centre des Sciences du Goût et de l'Alimentation, AgroSup Dijon, CNRS, INRAE, Université Bourgogne Franche-Comté, Dijon, France

⁴ Department of Nutritional Sciences, Faculty of Medicine, University of Toronto, Toronto, ON M5S 1A1, Canada

\$ Partners of the International Research Network Food4BrainHealth

* Corresponding author

ABSTRACT

Exposure to diets deficient in n-3 PUFAs decreases DHA throughout the cell membranes of the body. In order to determine more precisely whether a local decrease in DHA can alter synaptic plasticity, we developed an original transgenic approach that aims to decrease the bioavailability of DHA to neurons in restricted areas of the brain. For this purpose, we chose to administer a cre-mcherry adenovirus in the nucleus accumbens (NAC) of mice floxed for the gene of the enzyme ELOVL2, an elongase crucial in DHA synthesis. ELOVL2 is predominantly expressed by astrocytes which generate DHA that is then distributed to neurons. Thus, inhibition of ELOVL2 synthesis in astrocytes should be accompanied by a decrease in DHA in adjacent neurons. Patch-clamp electrophysiology measurements reveal for the first time that inhibition of astrocytic ELOVL2 alters the intrinsic properties of nearby neurons. In this case, we found a decrease in the excitability threshold of neurons and an increase in the amplitude of spontaneous activities. This suggests an alteration of the neuronal electrophysiological properties, in a context of astrocytic ELOVL2 inhibition.

1. INTRODUCTION

The brain contains large amounts of polyunsaturated fatty acids (PUFAs) (Bazinet and Layé, 2014), in particular docosahexaenoic acid (DHA) and arachidonic acid (AA) from the n-3 and n-6 families respectively. Several bodies of evidence collected in humans and animal models pinpoint that the alteration of brain PUFA metabolism is associated to altered emotional behavior and neuronal plasticity (Bazinet et al., 2020; Bazinet and Layé, 2014; Di Miceli et al., 2020). Although the exact mechanisms linking brain PUFAs and behavior are not completely understood, several data obtained in dietary animal model aiming at disturbing the level of n-3 and n-6 PUFAs in the brain, have revealed that the synaptic plasticity of medium spiny neurons (MSN) of the nucleus accumbens (NAc) is particularly altered when DHA and AA levels are changed at this level (Di Miceli et al., 2020; Ducrocq et al., 2020; Lafourcade et al., 2011; Lin et al., 2020; Manduca et al., 2015). In addition, altered synaptic plasticity in the NAc triggered by a chronic stress or n-3 PUFA dietary deficiency is responsible of emotional behavior alterations (Bosch-Bouju et al., 2016; Lafourcade et al., 2011; Manduca et al., 2015) and restored when mice are fed with a diet rich in DHA (Di Miceli et al., 2022; Larrieu et al., 2014). Altogether, these results strongly pinpoint the tight link between PUFA metabolism and synaptic plasticity in the NAc and emotional behavior. However, PUFA metabolism alteration was mainly triggered by dietary approaches, which impact PUFA metabolism at the level of the whole organism. In order to more precisely target PUFA metabolism in the NAc, we developed a mouse model with elongase (*elovl*)2 knock-out in NAc astrocytes. DHA and AA metabolism requires successive elongation and desaturation steps of their respective precursors α -linolenic acid (LNA) and linoleic acid (LA) (Jakobsson et al., 2006). In humans, *Elovl2* single nucleotide polymorphism (SNP) has been reported to alter plasmatic levels of n-6 and n-3 PUFAs (Tanaka et al., 2009). In addition, *elovl2* knock-out mice display strong impairment in DHA and AA metabolism in the brain, suggesting that this enzyme is key to PUFA homeostasis (Pauter et al., 2014; Talamonti et al., 2019). *Elovl2* is expressed in astrocytes, which are key cells in the regulation of synaptic plasticity (Human Protein Atlas) and have been shown to be crucial in the brain metabolism of DHA (Williard et al., 2001). However, whether the alteration of *elovl2* expression in astrocytes alters PUFA metabolism and neuronal activity is unknown. In addition, the differences according to sex have never been addressed.

To further gain insight in whether and how local disturbance of PUFA homeostasis in the NAc alters MSNs electrophysiological properties and/or emotional behavior, we generated a mouse model with *elovl2* genetic ablation in the NAc astrocytes. Then PUFA levels and MSNs electrophysiological properties were measured in the NAc and emotional behavior was assessed using a battery of tests in both male and female. Overall, no differences in PUFA metabolism was detected in the NAc of *elovl2* deficient astrocyte male and female mice. Alterations of some emotional parameters were detected in the KO male and female mice. In addition, electrophysiological properties of MSNs were profoundly

altered, suggesting that *elovl2* ablation in astrocytes impacts adjacent neurons in the NAc. However, the mechanisms underlying this effect remain to be understood.

2. MATERIAL AND METHODS

2.1. ANIMALS

All experiments were performed according to criteria of the European Communities Council Directive 2010/63/EU for animal experiments and were approved by the French Ministry of Research and the local ethical committee for the care and use of animals (N°APAFIS #17200 and #35867).

C56/BL6 mice *Elov12*^{lox/lox} were obtained from C Magnan (ELOVL2 IR00005097/K5097). AAV5/2-GFAP-mcherry-Cre expressing Cre recombinase gene under astrocyte GFAP promoter and AAV-5/2-GFAP-mCherry were purchased from the ETH Zurich (Zurich, Switzerland) and injected into each male and female *Elov12*^{lox/lox} mouse NAc.

Animals were housed in group of 6-9 animals in polycarbonate cages in an air-conditioned (22 +/- 1°C) colony room with a 12: 12 light/dark cycle according to their sex. Animals had *ad libitum* access to food and water and were weighed once a week. All mice were fed with a chow diet.

In total, 42 mice were used (20 males and 22 females). Before the virus injection, mice were genotyped using Ef/ER primers to discriminate WT, floxed homozygotes, heterozygotes and recombined as previously described (Birling et al., 2012).

The control group consisted of male and female *Elov12*^{lox/lox} mice injected with a control virus without cre expression (ctrl males; n=10 and ctrl females; n=11); the KO *elovl2* group consisted of male and female injected with the virus expressing the cre, the synthesis of *Elov12* is knock down in the astrocytes (KO *Elov12* group) (KO *Elov12* males; n=10 and KO *Elov12* females; n=11). All virus injections were performed in male and female mice at 6 weeks old. A first cohort was used for behavioral, electrophysiological or PUFA profile assessment in the NAc or immunohistochemistry. The second cohort was used for electrophysiological and RNAscope assessment in the NAc. Experiments were performed between 6 and 8 weeks after the intra-NAc administration of the control or cre-virus.

2.2. VIRAL PRODUCTION

Adeno-associated virus serotype 5/2 expressing the cre (AAV-5/2-hGFAP-mCherry-iCre-WPRE-hGHp(A)) (6×10^{12} genomes/mL, working dilution 1:10) was produced by the viral production facility of the ETH Zurich (Zurich, Switzerland). Control AAV-5/2-hGFAP-mCherry-WPRE-hGHp(A) (6×10^{12} vg/mL) was produced by the viral production facility of the the ETH Zurich (Zurich, Switzerland).

2.3. STEREOTAXIC INJECTION

Animals were anesthetized by inhalation of isoflurane (5-6% v/v ambient air) before being installed in a stereotaxic setting. The animals are maintained under isoflurane throughout the duration of the surgery (1-2% v/v) and on a heating mat to maintain body temperature at 37.5%. They received subcutaneous injection of analgesics (125µL / animal of Buprenorphine diluted at 1/100 in NaCl 0.9%, final dose at 0.05 mg/kg) 30 minutes before the induction of anesthesia. The eyes of animals are protected from desiccation by application of ophthalmic protection gel (Liposic 2mg/g).

The virus was injected into each hemisphere (0.5µL / hemisphere) with a flow rate of 0.1 µL / min using a Hamilton syringe in the nucleus accumbens (Nac) (L=1.56, AP=1.8, V=-4, in mm). The injection needle was carefully removed after 5 min waiting at the injection site and 2 min waiting half way to the top. Viscous xylocaine was applied to the wound. The animals received a subcutaneous injection of physiological saline (0.6 ml) to avoid dehydration in the first hours of his awakening as well as an injection of a nonsteroidal anti-inflammatory drug and analgesic CARPROFELICAN 50 mg/mL, diluted to 100th, 250 µL/animal). Animals were then placed in a clean cage on a heated and monitored mat for up to 6 hours after full awakening (resumption of motor activity). Animals are monitored twice daily for 3 days after surgery.

2.4. BEHAVIORAL TEST

Behavioral tests were conducted in both ctrl and KO *elovl2* mice 6 weeks after virus injection. Mice were weighted once a week since surgery. Mice were scored in behavioral tests performed in the light phase (between 8:00 AM and 11:00 AM). Mice were handled 5 min every day for 2 weeks before the initiation of experiments.

Anxiety-related tests were realized including Open Field test (10 min, 50 Lux), a light dark test (8 min, 300 Lux) and an EPM test (5min, 15 Lux). Between each experimental run, apparatus was cleaned to avoid olfactory disturbance. A video tracking system was used (SMART system; San Diego Instruments) to analyse the time spent in the different zone during 10 minutes of recording (Lafourcade et al., 2011; Larrieu et al., 2014).

From results obtained, an anxiety score is calculated for each animal based on normalized scores for each parameter measured on the behavioural tests (Time spent in the center of OF, total distance in the open field, time spent and number of entries in the light zone of the LD, time spent and number of entries in the open arm of the EPM, head dippings in the EPM).

2.5. ELECTROPHYSIOLOGY

Ex-vivo patch-clamp recordings were performed on brain slices from *Elov12* mice, as previously described (Berland et al., 2020; Lafourcade et al., 2011; Zemdeg et al., 2019)

Briefly, intracardiac perfusion was done during euthanasia (exagon/lidocaine: 300/30 mg/kg, i.p) with approximately 20ml of Cold NMDG solution to evacuate the brain of all blood and cool it quickly. NMDG solution is consisting of (in mM) : 1.25 NaH₂PO₄, 2.5 KCl, 7 MgCl₂, 20 HEPES, 0.5 CaCl₂, 28 NaHCO₃, 8 D-glucose, 5 L(+)-ascorbate, 3 Na-pyruvate, 2 thiourea, 93 NMDG, and 93 HCl 37%; pH: 7.3–7.4; osmolarity: 305–310 mOsm.

Sagittal striatal slices (350 µm) were prepared with a vibrating blade microtome (VT1000S, Leica Microsystems, Germany) in an ice cold oxygenated NMDG solution. Slices were placed 7 minutes in oxygenated NMDG at 32°C, then 50 minutes at room temperature in oxygenated artificial cerebrospinal fluid (ACSF) containing (in mM): 125 NaCl, 2.5 KCl, 1.25 NaH₂PO₄, 2.0 CaCl₂, 1.0 MgCl₂, 25 NaHCO₃, and 25 glucose (osmolarity 308 ± 3 mOsm) and recordings were started after.

Pipette resistance was typically between 4 and 7 MΩ when filled with a potassium gluconate-based intracellular solution, consisting of (in mM): K-gluconate 128, NaCl 20, MgCl₂ 1, EGTA 1, CaCl₂ 0.3, Na₂-ATP 2, Na-GTP 0.3, cAMP 0.2, and HEPES 10, pH = 7.35 (osmolarity 296 ± 3.8 mOsm). Pipette offset was zeroed before each recording.

Medium Spiny Neurons (MSN) of the NAc were visualized under direct interference contrast with a BX51WI microscope (Olympus, Tokyo, Japan), mounted on an air table (TMC, Saratoga Springs, NY, USA) and under a Faraday cage, with an upright microscope, a 40× water immersion objective combined with an infra-red filter, a monochrome CCD camera (Roper Scientific, Vianen, The Netherlands), and a PC-compatible system for analysis of images as well as contrast enhancement. Only data from MSNs near fluorescent astrocytes (mCherry) were included in the present study.

Membrane current and potential were monitored using Multiclamp700B and Digidata 1440A by Axon Instrument (Molecular Devices, San Jose, CA, USA). A concentric bipolar electrode (Phymep, Paris, France) was placed on afferent fibers to evoke EPSCs (at 0.1 Hz), recorded in MSN under voltage-clamp configuration with membrane potential clamped at –70 mV. Current over voltage (I/V) curves were acquired in I = 0 (free) current-clamp mode. All data were sampled at 20 kHz and filtered at 1 kHz. Series resistance was measured throughout the experiment with a –5 mV step lasting 50 ms. The active and passive electrophysiological properties of MSNs were calculated according to and consistent with a previous study (Di Miceli et al., 2022).

2.6. FATTY ACID PROFILE

Briefly, fatty acids from the prefrontal cortex and the nucleus accumbens were analysed as previously described (Delpech et al., 2015; Labrousse et al., 2012; Madore et al., 2014). Fatty acids composition of the PFC and NAc is expressed as the percentage of total fatty acids.

2.7. IMMUNOHISTOCHEMISTRY

Mice were perfused with PBS (n=2-6 animals/condition). Each brain was removed, postfixed in 4% paraformaldehyde overnight at 4°C, cryoprotected in 30% sucrose at 4°C and frozen in isopentane to be stored at -80°C. Brains were sectioned on a cryostat at 40 µm free-floating coronal sections and stored at -20°C in cryoprotectant solution. After washing off the cryoprotectant solution, slices were incubated 1h at room temperature in PBS blocking solution containing 5% Donkey serum and 0.3% Triton X-100, and immunostained with primary antibodies overnight at 4°C in PBS/5% Donkey serum/0.3% Triton X-100 (Rabbit-anti GFAP antibody (1 :1000 ; Dako Z0334), as an astrocytic marker and Goat-anti RFP antibody (1 :500 ; Rockland 200-101-379) to detect mCherry signal. Slices were then washing in PBS and incubated 2h at rt with secondary antibody in PBS/5% Donkey serum/0.3% Triton X-100 (Donkey-anti-rabbit Alexa Fluor 488 antibody (1 :1000 ; life technologies A21206) or Donkey-anti-Goat Alexa Fluor 647 antibody (1 :1000 ; life technologies A21447). Slices were then washed in PBS and mounted with UltraCruz® Hard-set Mounting Medium with Dapi (Santa Cruz Biotechnology sc-359850). Images were captured using with a Nanozoomer using a 20x objective (pixel size 0.454µm-Bordeaux Imaging Center, HAMAMATSU). Positive cells were quantified in the NAc shell (n=2-5 slices/animal ; Bregma 0.50mm-1.78mm) using Image-J ([National Institutes of Health](#)). Area of the quantified region has been measured and the data are presented as colocalisation of GFAP and mCherry staining.

2.8. RNASCOPE *IN SITU* HYBRIDIZATION (ISH) COMBINED WITH IMMUNOHISTOCHEMISTRY (IHC)

Mice were deeply anesthetized and transcardially perfused with phosphate buffered saline (PBS). After the perfusion, brains were removed, post-fixed in 4% paraformaldehyde (PFA) overnight (ON) at 4°C and cryoprotected in 30% sucrose ON at 4°C. Free-floating frozen coronal cryostat slices (40 µm) were collected in a cryoprotectant solution. Before the experiment, free-floating sections were mounted on Superfrost Plus microscope slides (Fisher Scientific). Several steps of air drying (1h), baking at 60°C (1h) and fast dipping in water were necessary to ensure the adhesion of the sections to the slides. Then, tissue sections were post-fixed 1h in 4% PFA at 4°C, followed by dehydration in a ethanol series. The RNAscope mRNA-staining steps was carried out as per the manufacturer's instructions for the RNAscope Multiplex Fluorescent V2 Assay (Biotechne, #323100). Briefly, tissue sections were treated with H₂O₂ for 10 minutes at RT and incubated in the Target Retrieval reagent 1X maintained at a boiling temperature for 5 minutes. Sections were then digested with protease III at 40°C for 30 minutes in a HybEZ hybridization oven (ACD, Hayward, CA), washed, followed by an incubation with the elovl2 probe at 40°C for 2h. Probe targeting the mRNA transcripts of ELOVL2 (target region : base pairs 1697-2808 of *Mus musculus* Elongation Of Very Long Chain Fatty Acids-Like 2, NM_019423.2, #542711-C3) was designed by ACD (a « channel 3 » probe). The channel 3 probe Elov12 was diluted at 1:50 in the probe diluent (Biotechne, #300041) prior to application on the

tissue sections. The bacterial gene *dapB* (dihydrodipicolinate *B. subtilis* reductase) was used as negative control to assess background signals. Amplification and detection steps were performed by adding the RNAscope Multiplex FL v2 HRP-C3 revealed by a TSA reaction using Opal 690 reagent pack (1/800 ; 30 minutes at 40°C ; Akoya Biosciences ; #FP1497001KT).

After processing for fluorescent ISH, an anti-GFAP and anti-RFP immunofluorescence was carried out. Sections were post-fixed 10 minutes at RT, then washed and incubated in a blocking solution of 5% donkey serum, 0.3% Triton X-100 prepared in PBS for 30 minutes at RT. Sections were then incubated with a mix of primary antibodies overnight at 4°C : a goat polyclonal anti-RFP (1 :500, Rockland, #200-101-379) and a rabbit polyclonal anti-GFAP (1 :500, DAKO, #Z0334). After several washes, sections were placed, for 2 hours, at RT, in the dark, with a mix of secondary antibodies : donkey anti-goat Alexa Fluor 555 (1 :500, Fisher Scientific, #10246402) and donkey anti-rabbit Alexa Fluor 488 (1 :500, Fisher Scientific, #10424752). Stained slides were mounted with ultraCruz hard-set mounting medium with DAPI (Clinisciences, #sc-359850).

Microscopic imaging and statistical analysis: images were acquired using a Zeiss inverted Axio Observer fluorescent microscope (Carl Zeiss). Sections were analysed to examine the deletion of mRNA *Elovl2* in the astrocytes at the level of the NAc of transfected mice. Image analyses and counting were performed in 1 section of 4 mice in each condition.

Quantification of the number of labelled dots within the tissue. Each dot represents one RNA molecule and thus, the number of dots is indicative of the number of RNA molecules present. Scoring of RNAscope/immunofluorescence staining was done manually.

2.9.STATISTICAL ANALYSIS

All statistical tests were performed with GRAPHPAD PRISM 9 software. Significance was set at $\alpha = 0.05$. All values are reported as mean \pm standard error of the mean (SEM) and represented as histograms or with box and whiskers representation from min to max. Data analysis was performed using one-sample t-tests, two- or three-way ANOVA, followed by post hoc tests if appropriate. For the RNAscope analysis, difference between the mice injected with control virus and the one injected with KO *Elovl2* virus were compared using an unpaired t-test. A P value of <0.05 was considered statistically significant. Data are presented as the mean value and error bars represent SEM.

Supplemental Table S1 presents all statistical analysis results performed in the present study.

3. RESULTS

First, the impact of the administration of the AAV-cre specific for astrocyte in the NAc of male mice, on *elovl2* mRNA expression was assessed using RNAscope. This technic is giving us the opportunity to localize both astrocytes (GFAP) and the expression of *elovl2* RNA molecules (white dots) (**Fig. 2.A**). The hippocampus has been used as the control structure (away from the administration site). Quantitative image analysis of RNAscope data for *Elov12* and double immunofluorescence for RFP and GFAP proteins showed that expression of *Elov12* is reduced by 50 % in astrocytes targeted by the Cre+ virus (Unpaired t-test, $t=3,995$, $df=6$, $p<0,01$) (**Fig. 2.B**).

Second, we assessed using immunohistochemistry the number of astrocytes co-labelled with mcherry, used as a proxy of the virus expression. In order to validate the injection site and to see if the virus was targeting astrocytes and in which proportion in the NAc. In male mice, no significant differences were observed (**Fig. 3**). In females, we only have preliminary datas presented in supplementary datas (**Fig. 8**).

PUFA profile is not altered in the NAc of *Elov12* KO male and female mice

Then, we evaluated if the diminution of *Elov12* expression in the astrocyte of the NAc was associated to altered PUFA profile in the NAc of control or cre AAV (KO *Elov12*) male and female mice (**Fig. 1**). The same measurements were performed in the prefrontal cortex (PFC), used as a control brain structure. No significant changes in saturated fatty acids (SFA), monounsaturated fatty acids (MUFA) and PUFA level were measured in the NAc and PFC of ctrl and KO *Elov12* (**Fig. 4 and 5**).

Individual emotional behaviors are slightly altered in *Elov12* KO male and female mice, with no effect on the anxiety score

In order to investigate whether KO *Elov12* induced changes in emotional behavior, we performed Open Field (OF), Light Dark (LD) and Elevated Plus Maze (EPM) tasks in male and female mice (**Fig. 6**). No significant differences were measured in behavioral performance of male and female mice under study in the OF test (**Fig. 6A**). Interestingly, KO *Elov12* male, but not female, mice display some anxiety-like behavior, as revealed by the significant time spent in the light area of the LD test (Unpaired t-test, $t=2.637$, $df=12$, $p<0.05$) (**Fig. 6B**). In addition, KO *Elov12* female mice have more head dippings when placed in the EPM test (Unpaired t-test, $t=2.260$, $df=12$, $p<0.05$) (**Fig. 6C**). The calculation of the anxiety score did not reveal significant differences between control and KO *Elov12* male and female mice (**Fig. 6D**).

MSN intrinsic electrophysiological properties are altered in *Elov12* KO male and female mice

To reach the sufficient number of animals required to perform statistical analysis, results from male and female were pooled. A significant effect of the astrocytic Elov12 KO was measured on the voltage over current relationships (Two way ANOVA, voltage effect : $F(23,529)=167.1$, $p<0.001$, virus effect : $F(1,23)=4.988$, $p<0.05$, interaction : $F(23,529)=167.1$, $p<0.001$) (**Fig. 5B**), together with altered rheobase compared to control animals (Unpaired t-test, $t=3.442$, $df=22$, $p<0.01$) (**Fig. 5D**). In addition, the number of action potentials generated during supra-threshold current applications were altered in MSNs of KO elvol2 (Two way ANOVA, current effect : $F(6,132)=29.03$, $p<0.001$, virus effect : $f(1,22)=2.434$, ns, interaction : $F(6,132)=5.046$, $p<0.001$) (**Fig. 7E**). However, there was no significant effect on the resting membrane potential (**Fig. 7C**). We also recorded spontaneous excitatory post synaptic current (sEPSC). MSNs from KO Elov12 display a significant decrease of the amplitude of these sEPSC (Unpaired t-test, $t=15.03$, $df=882$, $p<0.001$) (**Fig., 7G**), but not of the interevent interval (**Fig. 7F**) or the frequency (**Fig. 7H**). Finally, the probability to trigger a spike (in %) in recorded MSNs following increasing cortical stimulations is not significantly higher in KO Elov12 animals (**Fig. 7J**).

4. DISCUSSION

In this second part of our study, we focused on the local modulation of fatty acids levels. After injection of the virus into the NAc, immunohistochemical analyses of the colocalization of the GFAP and mCherry markers allowed us to confirm that cre is expressed predominantly in astrocytes. Then, using an RNAscope approach, we were able to estimate the number of astrocytic cells targeted by the virus and, among these infected cells, to quantify the expression level of elov12 transcripts. Administration of AAV-5/2-GFAP-re/mCherry in the NAc of male and female ELOVL2lox/lox mice decreases elvol2 expression by 50% at this level, but not in the hippocampus, used as a control structure. Analyses of lipid profiles in Nac and PFC show that inhibition of astrocytic elov12 synthesis did not induce differences in the level of SFAs, MUFAs or PUFAs in the NAc of males and females. This is in contrast to what has been observed in total KO models for Elov12, which show changes in PUFA levels, including increased levels of n-3 DPA and decreased DHA in the brains of KO mice (Gregory et al., 2013; Pauter et al., 2014; Talamonti et al., 2019). Our results could be explained by the fact that the changes at the astrocyte level are too small to be detected at the scale of the whole structure. But it could also be that alternative pathways take over for endogenous DHA synthesis, as is the case in zebrafish liver (Liu et al., 2020). Indeed, elov12^{-/-} zebrafish do not show accumulation of n-3 DPA but an increase in the substrate of the delta 4 desaturase pathways, EPA, suggesting that the delta 4 pathway is an alternative for DHA synthesis (Liu et al., 2020). Furthermore, the deletion of elov12 is not complete, which may explain the absence of changes in PUFA levels in NAc. Behavioural analyses revealed alterations in emotional behaviour on parameters that differed in Elov12 knockout animals according to sex. Indeed, we were able to observe that Elov12 knockout males spend

significantly more time in the Light Dark zone than control animals. The Light Dark test confronts mice with an extremely anxiety-provoking situation that consists of exposure to a very brightly lit area. Our results suggest that male Elov12 KO mice are less anxious than control animals. Secondly, we found that female Elov12 KO mice performed less head dipping in the elevated cross maze test. This parameter consists of counting the number of times the animal engages its head and upper body above the void. Elov12 knockout females thus appear to exhibit anxiety-like behaviour compared to control animals.

Finally, we were able to observe changes in neuronal excitability. Indeed, neurons recorded in the vicinity of fluorescent astrocytes show a lower rheobase and a decrease in the number of action potentials. Analysis of the spontaneous activity of excitatory postsynaptic currents shows that the amplitude of these activities is decreased in Elov12 KO animals but not the frequency or the interval between events. To our knowledge, there are no studies that have analysed the neuronal properties under astrocytic control in the NAc. Neuronal activity in the NAc is regulated by various neurotransmitters or neuromodulators released from the afferents, notably GABAergic ones. Astrocytes are known to express glutamate transporters (GLAST and GLT-1), as well as GABA transporters (GAT1-3) (Danbolt, 2001; Gadea and López-Colomé, 2001a, 2001b). Partial inhibition of elov12 expression in the astrocyte could modify the expression of GABA and GLUT transporters at this level. To better understand how changes in elov12 expression by the astrocyte modify neuronal properties, studies of astrocytic reuptake that modulate the intensity and duration of activation of receptors located at the pre- or postsynaptic level (Tzingounis and Wadiche, 2007), limit the activation of extra-synaptic receptors (Huang and Bergles, 2004) or limit the diffusion of neurotransmitters to neighbouring synapses (Arnth-Jensen et al., 2002) are necessary.

In summary, the results obtained in the Elov12 KO model show for the first time that altering astrocytic elov12 synthesis alters emotional behaviour on gender-specific parameters and alters the electrophysiological properties of MSNs in the NAc. However, further analysis is needed to better understand the mechanisms involved in these modifications

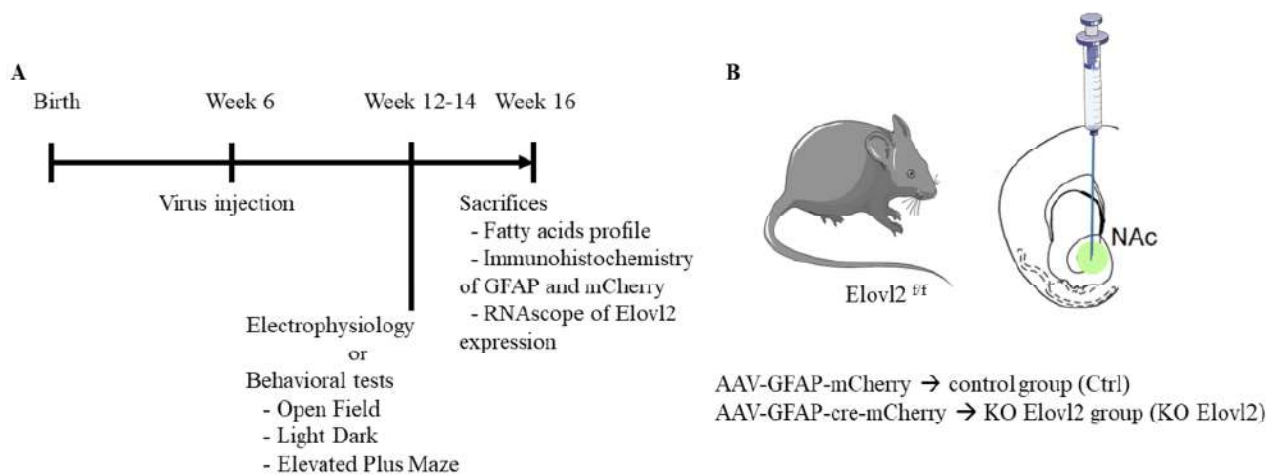


Figure 1 : Representation of experimental design. (A) Between 6 and 8 weeks after viral injection, behavioral tests and electrophysiological recordings are performed before biochemical analysis. (B) 6 weeks after birth, viral injection of control virus (ctrl) and cre-virus (KO Elov12) under GFAP promoter and expressing mCherry in C57Bl6j Elov12 floxed mice were done in the Nucleus Accumbens (NAc).

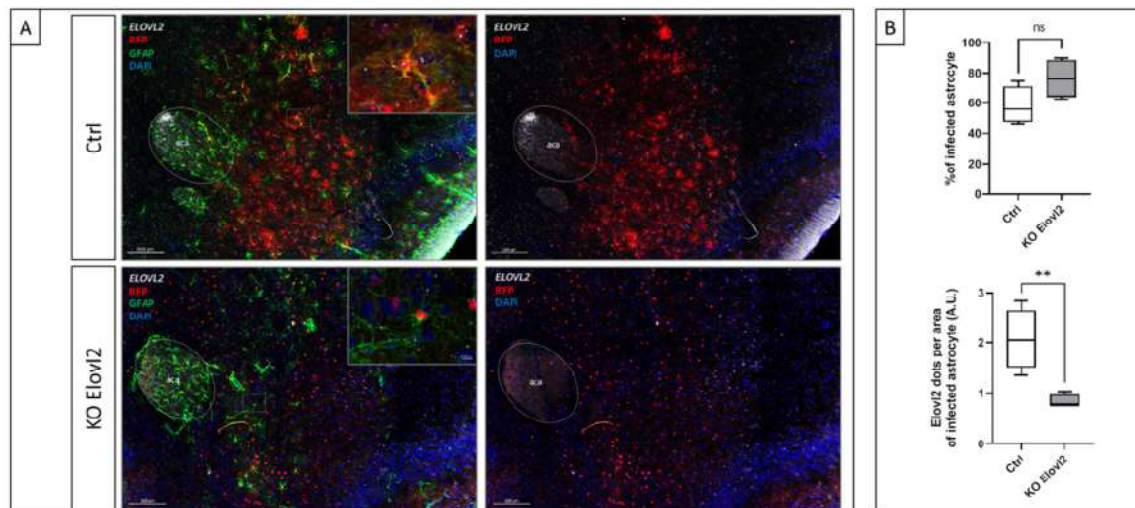


Figure 2 : Decrease of the expression of ELOVL2 in the astrocytes of mice injected with Cre+ virus in the Nac. (A) : Representative images of mice Elov12 lox injected with ssAAV-5/2-hGFAP-mCherry-WPRE-hGHp(A) (Cre-) or ssAAV-5/2-hGFAP-mCherry_iCre-WPRE-hGHp(A) (Cre+) in the Nac. Simultaneous detection of one target gene *ELOVL2* (white dots) by RNAscope ISH and two proteins RFP (red) and GFAP (green) in mice injected by Cre- or Cre+ virus in the Nac. Each dot (white) represents one RNA molecule of *ELOVL2*. The dotted white circle represents the anterior commissure, anterior part (aca). White dotted boxes are magnified. n=4 animals. Original magnification, x20. Scale bar = 200 μ m. (B) : Quantitative image analysis of RNAscope data for Elov12 and double immunofluorescence for RFP and GFAP proteins.

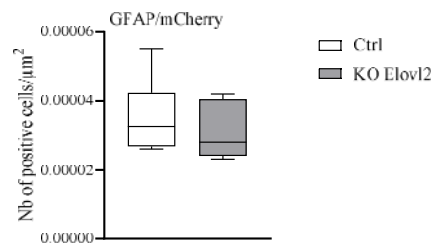
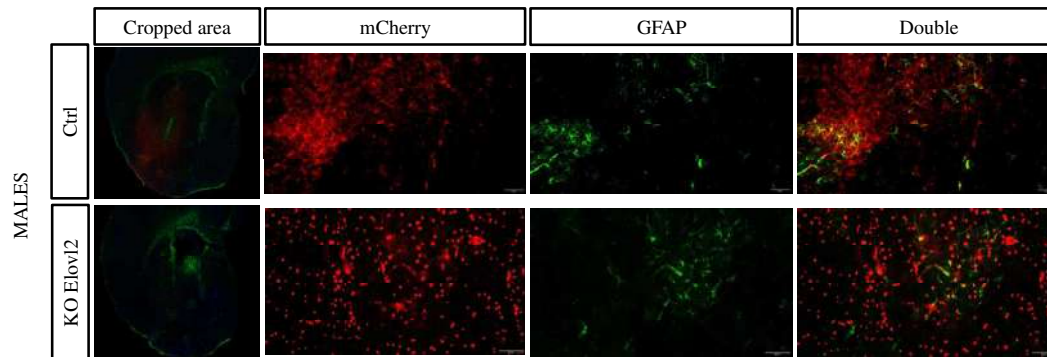


Figure 3 : Representative GFAP immunostaining in striatal area of mice injected with the control virus (ctrl) and the cre virus (KO Elov12). Scale bar, 100 μm . Quantification of the colocalisation between GFAP immunostaining and mCherry fluorescence. Values (box and whiskers plots) (ctrl n=6; KO Elov12 n=7) are plotted from minimum to maximum. One-Way ANOVA followed by Bonferroni test if the ANOVA is significant. * $p < 0.05$, ** $p < 0.01$, *** $p < 0.001$ Ctrl versus KO Elov12 mice.

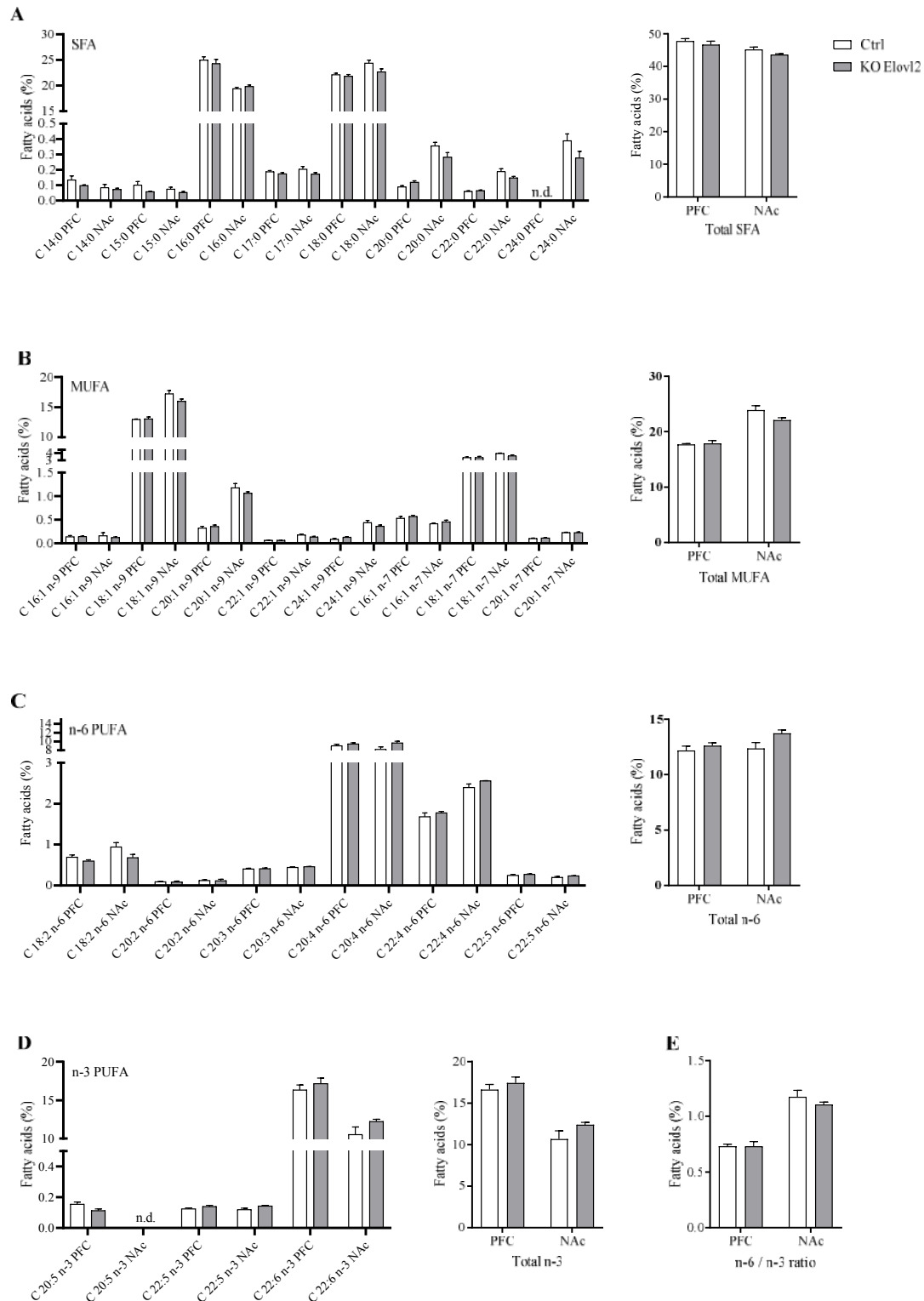


Figure 4 : Striatal fatty acids profiles of male mice from the control (Ctrl) virus injection or the KO for Elov12 (KO Elov12) condition on prefrontal (PFC) and Nucleus Accumbens (NAc) brain regions. (A) Saturated fatty acids (SFA) and total SFA. (B) Mono-unsaturated fatty acids (MUFA) and total MUFA. (C) n-6 polyunsaturated fatty acids (PUFA) and total n-6 PUFA. (D) n-3 PUFA and total n-3

PUFA. (E) n-6/n-3 ratio. n.d. = non detected. Results are expressed in % of total fatty acids in the hippocampus. Histograms represent mean \pm SEM (n=5/group). One-Way ANOVA followed by Bonferroni test if the ANOVA is significant. * p<0.05, ** p<0.01, *** p<0.001

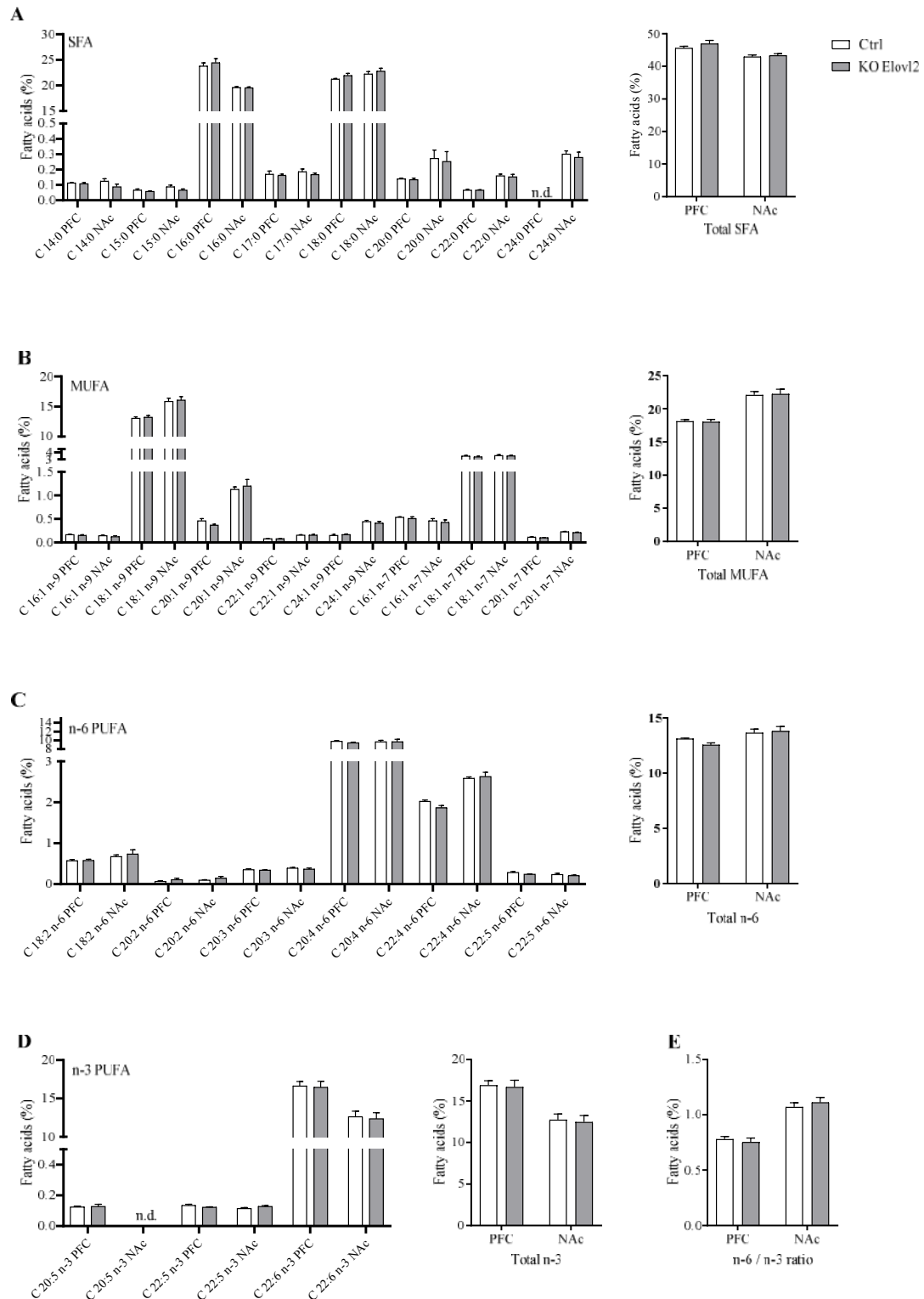


Figure 5 : Striatal fatty acids profiles of female mice from the control (Ctrl) virus injection or the KO for Elovl2 (Elovl2 $-/-$) condition on prefrontal (PFC) and Nucleus Accumbens (NAc) brain regions. (A) Saturated fatty acids (SFA) and total SFA. (B) Mono-unsaturated fatty acids (MUFA) and total MUFA. (C) n-6 polyunsaturated fatty acids (PUFA) and total n-6 PUFA. (D) n-3 PUFA and total n-3

PUFA. (E) n-6/n-3 ratio, n.d. = non detected. Results are expressed in % of total fatty acids in the hippocampus. Histograms represent mean \pm SEM (n=5/group). One-Way ANOVA followed by Bonferroni test if the ANOVA is significant. * p<0.05, ** p<0.01, *** p<0.001

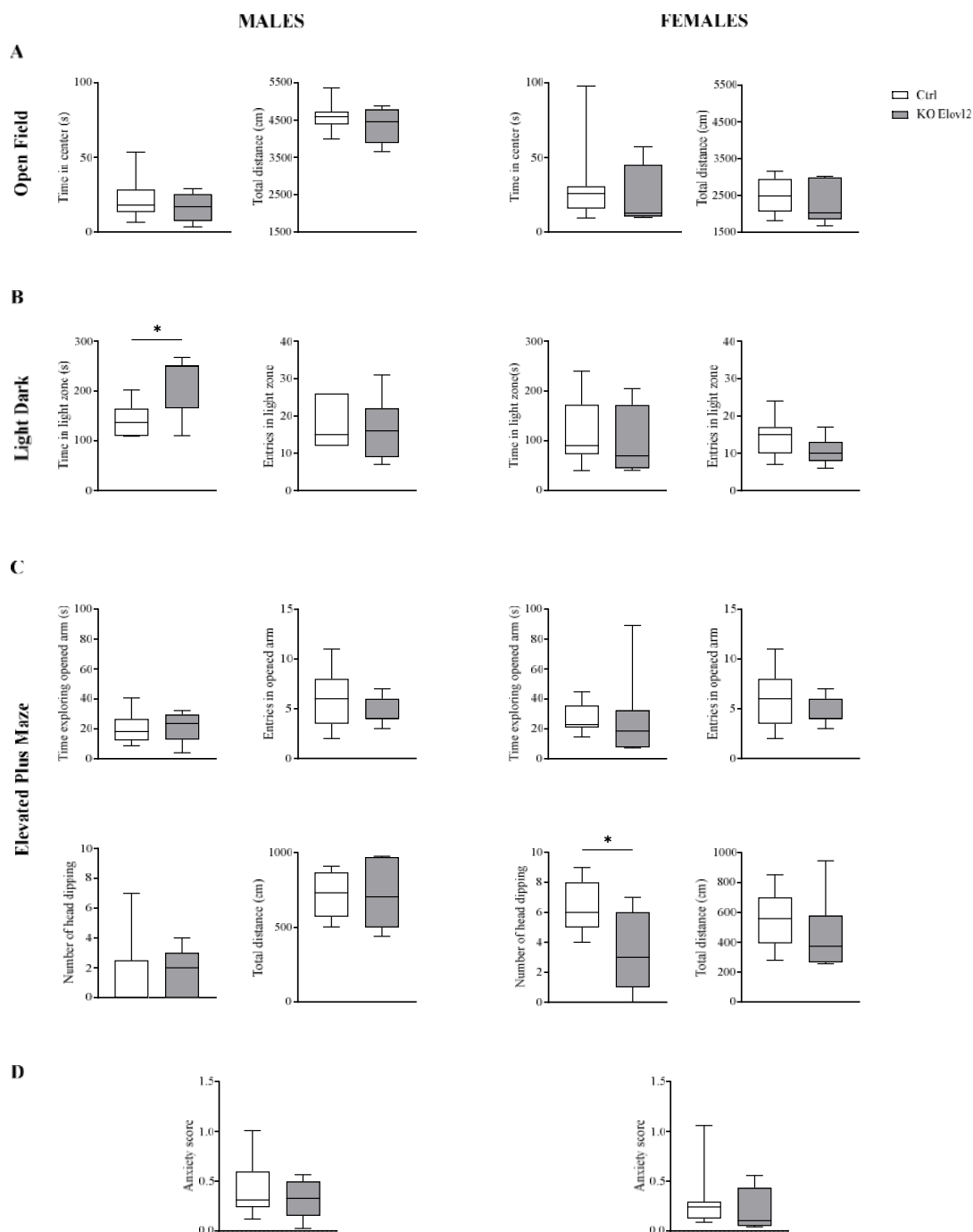


Figure 6 : Anxiety-like behavioral assessments in males and females control and KO Elov12 mice. **(A)** Open Field. **(B)** Light Dark. **(C)** Elevated Plus Maze. **(D)** Anxiety scores were calculated by normalizing and balancing 6 different behavior measurements. Values (box and whiskers plots) (n=7/group) are plotted from minimum to maximum. One-Way ANOVA followed by Bonferroni test if the ANOVA is significant. * p<0.05, ** p<0.01, *** p<0.001

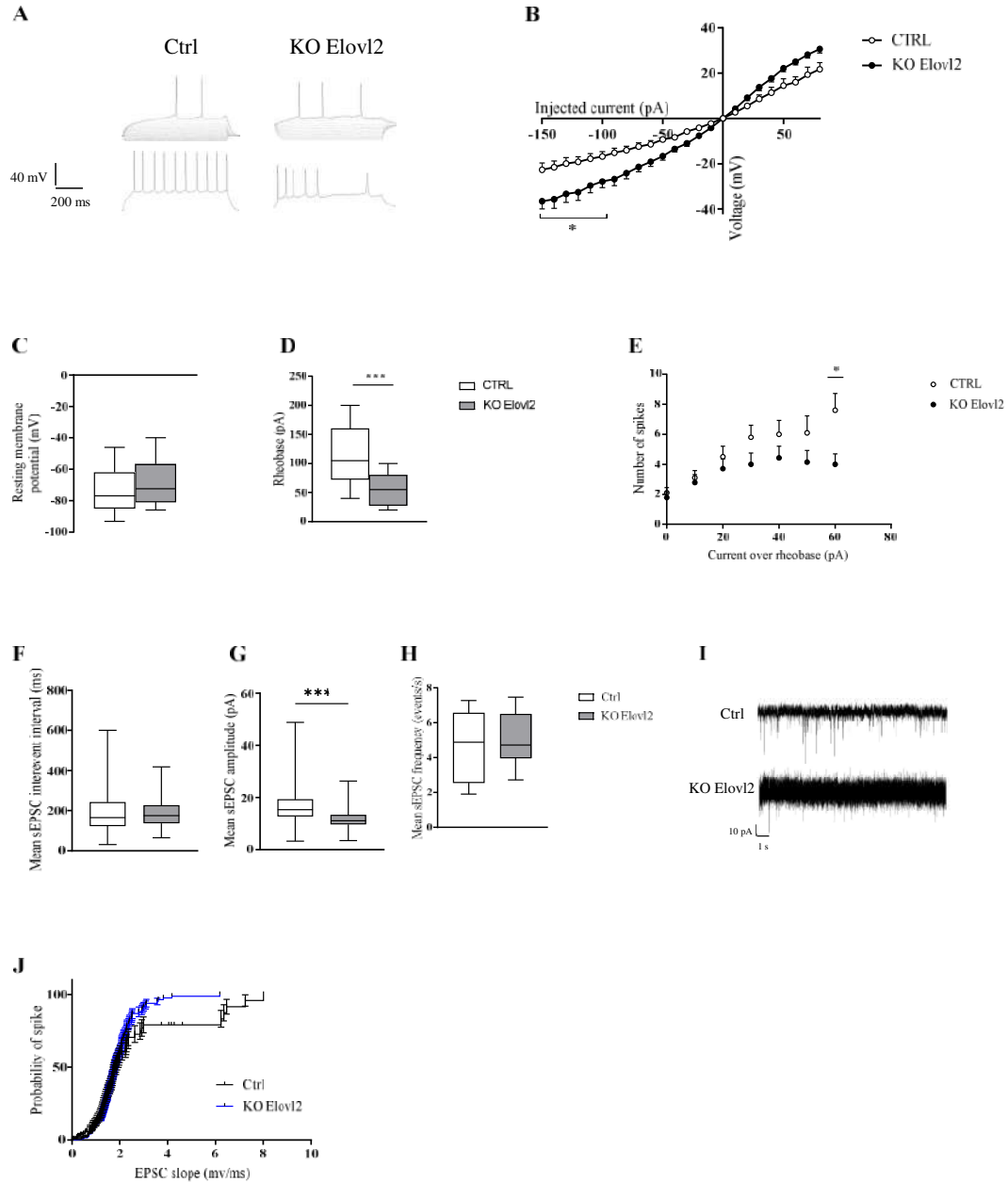


Figure 7 : Modulation of accumbal medium spiny neurons intrinsic electrophysiological properties. (A) Representative firing pattern. (B) Voltage over current (I/V) curve. (C) Resting membrane potential (RMP in mV). (D) Rheobase (in pA). (E) Number of action potential (AP) generated over rheobase current (I-F) relationship. (F-I) Quantitative summary of interevent interval (in ms, F), amplitude (in pA, G) and frequency (in events/s, H) illustrated by traces (I). (J) Curves indicate the probability to trigger a spike (in %) in recorded MSNs following increasing cortical stimulations in both conditions. (C-D-F-G-H) Values (box and whiskers plots) are plotted from minimum to maximum. One-Way ANOVA followed by Bonferroni test if the ANOVA is significant. * $p < 0.05$, ** $p < 0.01$, *** $p < 0.001$ Statistics: * $p < 0.05$ and ** $p < 0.01$ Ctrl versus KO Elov12 mice.

SUPPLEMENTARY DATA

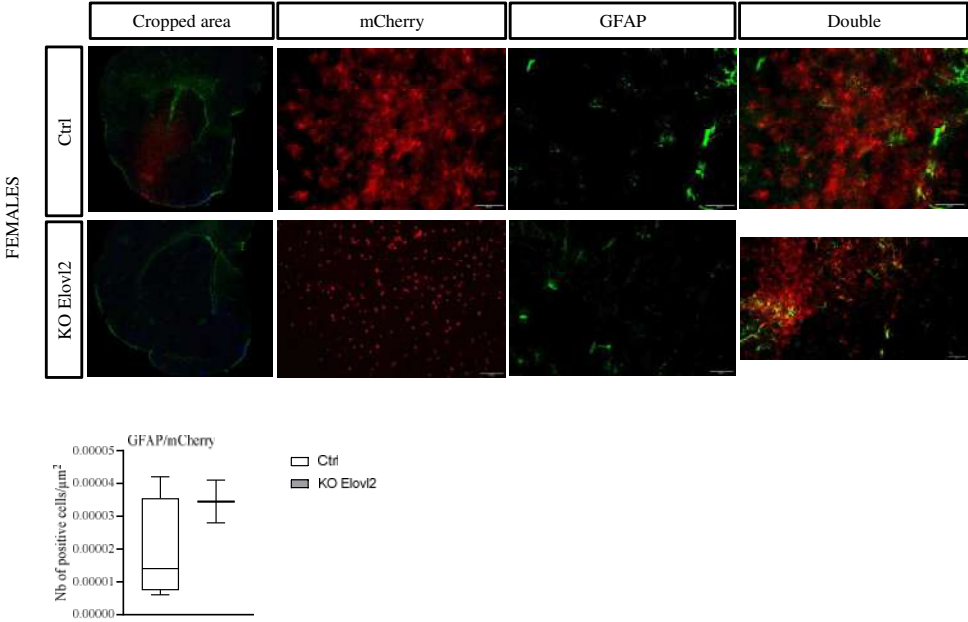


Figure 8 : Preliminary data of representative GFAP immunostaining in striatal area of female mice injected with the control virus (ctrl) and the cre virus (KO Elov12). Scale bar, 100 μm. Quantification of the colocalisation between GFAP immunostaining and mCherry fluorescence. Values (box and whiskers plots) (ctrl n=4; KO Elov12 n=2) are plotted from minimum to maximum.